Charging Demand of Plug-in Electric Vehicles: Forecasting Travel Behavior Based on a Novel Rough Artificial Neural Network Approach

Hamidreza Jahangir[1], Hanif Tayarani[1], Ali Ahmadian[2], Masoud Aliakbar Golkar[1], Jaume Miret[3], Mohammad Tayarani[4], H. Oliver Gao[4, *]

[1] K. N. Toosi University of Technology, Department of Electrical Engineering, Tehran, Iran

[2] University of Bonab, Department of Electrical Engineering, Bonab, Iran

[3] Polytechnic University of Catalonia, Electronic Engineering Department, 08034 Barcelona, Spain

[4] Cornell University, School of Civil and Environmental Engineering, Ithaca, NY 14853, United States

[*] Corresponding author

E-mail addresses: h.r.jahangir@email.kntu.ac.ir; haniftayarani@email.kntu.ac.ir; ahmadian@bonabu.ac.ir; Golkar@kntu.ac.ir; jaume.miret@upc.edu; mt789@cornell.edu; hg55@cornell.edu

ABSTARCT

The market penetration of Plug-in Electric Vehicles (PEVs) is escalating due to their energy saving and environmental benefits. In order to address PEVs impact on the electric networks, the aggregators need to accurately predict the PEV Travel Behavior (PEV-TB) since the addition of a great number of PEVs to the current distribution network poses serious challenges to the power system. Forecasting PEV-TB is critical because of the high degree of uncertainties in drivers' behavior. Existing studies mostly simplified the PEV-TB by mapping travel behavior from conventional vehicles. This could cause bias in power estimation considering the differences in PEV-TB because of charging pattern which consequently could bungle economic analysis of aggregators. In this study, to forecast PEV-TB an artificial intelligence-based method -feedforward and recurrent Artificial Neural Networks (ANN) with Levenberg Marquardt (LM) training method based on Rough structure - is developed. The method is based on historical data including arrival time, departure time and trip length. In this study, the correlation among arrival time, departure time and trip length is also considered. The forecasted PEV-TB is then compared with Monte Carlo Simulation (MCS) which is the main benchmarking method in this field. The results comparison depicted the robustness of the proposed methodology. The proposed method reduces the aggregators' financial loss approximately by 16 $/PEV per year compared to the conventional methods. The findings underline the importance of applying more accurate methods to forecast PEV-TB to gain the most benefit of vehicle electrification in the years to come.

Keywords: Plug-in electric vehicle; Travel behavior; Artificial neural network; Rough neuron; Smart charging.

1 Nomenclature

2 A. Indices

i	Index of input data
g	Index of output layer sample
j	Index of hidden layer sample
k	Index of iteration number
l	Index of plug-in electric vehicle
p	Index of node
q	Index of node
S	Index of layer number
t	Index of time
u	Index of equipment

3 B. Parameters

$B(p,q)$	Susceptance of transmission line between bus p and bus q
C_{inf}	Charging infrastructure cost
C_{eff}	Efficiency factor of the *l*-th PEV
$Cap_{bat,l}$	The capacity of *l*-th PEV's battery
$G(p,q)$	Conductance of transmission line between bus *p* and bus *q*
M	Total number of input data in Levenberg–Marquardt method
n_0	Total number of input data components
n	Total number of nodes
N_T	Total number of training neurons in Levenberg–Marquardt method
N_w	Total number of weights in Levenberg–Marquardt method
N_{w_L}	Total number of lower bound weights in Levenberg–Marquardt method
N_{w_U}	Total number of upper bound weights in Levenberg–Marquardt method
n_{pev}	Total number of PEVs
n_{eq}	Number of all equipment
nd	Total number of sample data
P_{max}^{u}	Maximum active power of equipment *u*
Q_{max}^{u}	Maximum reactive power of equipment *u*
SOC_{dep}	PEV's minimum SOC at departure time
$V_{\max}$	Maximum voltage of nodes
V_{min}	Minimum voltage of nodes
ρ_{chr}	Charging efficiency parameter
η_w	Training coefficient for weights
η_C	Training coefficient for context weights in recurrent network
η_ψ	Training coefficient for flexible activation function parameter

4 C. Variables

$Ca(t)$	Cost of active power at time *t*
$Cr(t)$	Cost of reactive power at time *t*
$d(k)$	Desired output in iteration *k*
$e_j^S(k)$	Error value for neuron *j* in layer *S* in iteration *k*

$e_{jM}(k)$	Error of neuron *j* for input data *M* in Levenberg–Marquardt method in iteration *k*
$e_{jM_L}(k)$	Error of lower bound neuron *j* for input data *M* in Levenberg–Marquardt method in iteration *k*
$e_{jM_u}(k)$	Error of upper bound neuron *j* for input data *M* in Levenberg–Marquardt method in iteration *k*
e_{L-M}(k)	Error vector in Levenberg-Marquardt method in iteration *k*
E	Total Sum square error
$E(k)$	Total Sum square error in iteration *k*
$f_j^s(k)$	Activation function for neuron *j* in layer *S* in iteration *k*
$H(k)$	Hessian matrix in iteration *k*
$I(k)$	Identity matrix in iteration *k*
$J(k)$	Jacobian matrix in iteration *k*
$La(t)$	Active load at time *t*
$Lr(t)$	Reactive load at time *t*
$net\ (k)$	Activation function input in iteration *k*
$net_j^s(k)$	Activation function input for neuron *j* in layer *S* in iteration *k*
$net_{Lj}^s(k)$	Lower bound of activation function input for neuron *j* in layer *S* in iteration *k*
$net_{Uj}^s(k)$	Upper bound of activation function input for neuron *j* in layer *S* in iteration *k*
$O^s(k)$	Output of layer *S* in iteration *k*
$O_j^s(k)$	Output of neuron *j* in layer *S* in iteration *k*
$O_U^s(k)$	Output of upper bound neuron for layer *S* in iteration *k*
$O_L^s(k)$	Output of lower bound neuron for layer *S* in iteration *k*
$O_{Uj}^s(k)$	Output of upper bound neuron *j* for layer *S* in iteration *k*
$O_{Lj}^s(k)$	Output of lower bound neuron *j* for layer *S* in iteration *k*
$P^u(t)$	Active power of equipment u at time *t*
$P_l^{chr}(t)$	Charging rate for PEV *l* at time *t*
$PEVa(t)$	PEV's active power at time *t*
$PEVr(t)$	PEV's reactive power at time *t*
$Plossa(t)$	Active power loss at time *t*
$Plossr(t)$	Reactive power loss at time *t*
$Q^u(t)$	Rective power of equipment *u* at time *t*
$Ra(t)$	Purchesed active power at time *t*
$Rr(t)$	Purchesed reactive power at time *t*
$SOC_{init,l}(t)$	SOC at initial time *t* for *l*-th PEV
$SOC_{dep,l}(t)$	SOC at departure time *t* for *l*-th PEV
$SOC_l(t)$	SOC at time *t* for *l*-th PEV
Tl_l	Trip length by *l*-th PEV
$Wa(t)$	Wind active power at time *t*
$Wr(t)$	Wind reactive power at time *t*
$w_j^s(k)$	Weight vector for neuron *j* in layer *S* in iteration *k*
$w\ (k)$	Weight vector for neuron *j* in layer *S* in iteration *k*
$W_{Uc}^S(k)$	Weight vector of upper bound context neurons in recurrent network in iteration *k*
$W_{Lc}^S(k)$	Weight vector of lower bound context neurons in recurrent network in iteration *k*
$W_U(k)$	Weight vector of upper bound neurons in iteration *k*
W_L(k)	Weight vector of lower bound neurons in iteration *k*

$W_{U_j}^S(k)$	Weight of upper bound neuron *j* in layer *S* in iteration *k*
$W_{L_j}^S(k)$	Weight of upper bound neuron *j* in layer *S* in iteration *k*
$W_{ij}^S(k)$	Weight vector between sample *i* of input layer and neuron *j* in hidden layer *S* in iteration *k*
$V(p,q,t)$	Line voltage between bus *p* and *q* at time *t*
$V_p(t)$	Voltage value for bus *p* at time *t*
X	Input data vector
X_C	Input data vector for recurrent network
X_i	Input data vector for sample *i*
Y_g	Output vector for sample *g*
$\widehat{Y_g}$	Desired vector for sample *g*
λ_j^S	Coefficient of upper bound neuron *j* for layer *S*
γ_j^S	Coefficient of lower bound neuron *j* for layer *S*
$\mu(k)$	Levenberg-Marquardt decision variable in iteration *k*
$\theta_{p,t}$	Voltage's angel of node *p* at time *t*
$\theta_{q,t}$	Voltage's angel of node *q* at time *t*
$\psi(k)$	Flexible activation function parameters in iteration *k*

D. Abbreviations

ANN	Artificial Neural Network
CEBP	Conventional Error Back Propagation
LM	Levenberg Marquardt
MAE	Mean Absolute Error
MAPE	Mean Absolute Percentage Error
MLP	Multi-Layer Perceptron
NHTS	National Household Travel Survey
NLP	Non-Linear Programming
OC	Operation Cost
PEV	Plug-in Electric Vehicle
PEV-TB	Plug-in Electric Vehicle Travel Behavior
R-ANN	Rough Artificial Neural Network
R-CEBP	Rough based Conventional Error Back Propagat
R-LM	Rough based Levenberg Marquardt
RR-LM	Recurrent Rough network with Levenberg Marquardt training method
RR-CEBP	Recurrent Rough network with Conventional Error Back Propagat training method
RR-ANN	Recurrent Rough Artificial Neural Network
RMSE	Root Mean Square Error

1. INTRODUCTION

1.1. Background and motivation

Transportation sector is the main source of the greenhouse gases (27%) and CO_2 (32%) (Fan et al., 2018) and many other criteria air pollutants in the U.S (US EPA, 2019). Worries over the pollution from fossil fuels in the transportation sector and concerns about cleaner production strategies have instigated the tendency to use Plug-in Electric Vehicles (PEVs) instead of the conventional internal combustion engines (Li et al., 2019; Tayarani et al., 2018b, 2018a). It is estimated that at least 10 percent of the US fleet will be replaced by electric vehicles by 2020 and their market share could reach 50 percent by 2050 (Mukherjee and Gupta, 2017). The addition of a great number of PEVs to the current distribution network poses serious challenges to the planning, controlling, and

operating of existing power systems(Aliasghari et al., 2018). In order to deal with the challenges posed by PEVs to power systems, several studies have been devoted to scrutinizing the optimal smart charging of PEVs. The PEVs charging demand should be forecasted and calculated for designing of smart charging strategies. More accurate forecasting methods would be also appreciated by the smart charging planners who are known as aggregators in this field. However, only a few available studies have exploiting precise PEV-Travel Behavior (PEV-TB) forecasting methods to determine the smart and efficient charging algorithms. Machine learning and artificial intelligence data-driven methods can forecast PEVs-TB using the previous data. Despite the benefits of the machine learning based approaches, they have been rarely applied in forecasting PEV-TB. This paper fills the gap in existing literature by introducing a new approach in forecasting charging demand of the PEV. In this paper an innovative approach is proposed to more precisely forecast the PEV-TB to generate more realistic travel pattern used in aggregator planning. Furthermore, this study includes the aggregator financial loss based on the error of forecasting the PEV-TB.

1.2. Literature review

With the recent increase in penetration of PEVs in the transportation fleet, it is indispensable to forecast the PEVs load demand on the electricity networks. In order to reach high accuracy in forecasting PEV's load, the characteristics of driver's behavior such as trip length, arrival time and departure time ought to be estimated precisely. Existing approaches to model PEV-TB can be classified into four categories. First, the Monte Carlo simulation (MCS) as the benchmarking method (Arias and Bae, 2016; Biswas et al., 2017; Mohseni-Bonab and Rabiee, 2017; Morshed et al., 2018; Neaimeh et al., 2015; Qian et al., 2011; Yu et al., 2015) is usually employed to generate numerous scenarios. Most existing studies (Sun et al., 2018; Wang and Infield, 2018; Yang et al., 2018) applied normal distribution function for estimating all the parameters which untimely reduces the accuracy of PEV-TB forecasting. Moreover, the problem's dimensions will expand significantly if the PEVs number is increased. Therefore, the numerous scenarios of MCS increase the computation time and make the algorithm unprofitable for the complex operation and planning procedures. The limited number of scenarios could also reduce the accuracy of the results (Ahmadian et al., 2018). Furthermore, the MCS method does not consider the correlation between the PEVs-TB parameters such as arrival time, departure time and trip length in the production of different PEV-TB scenarios. Thus, it is possible for the simulated travel data to be inconsistent. For instance, the travel time may not match with the arrival and departure times.

The models in the second approach use Markov chain theory to forecast PEVs load demand. For instance, Sun et al.,(Sun et al., 2018, 2016) has provided a conventional Markov based method to model PEV-TB. Estimating the transition matrix as the probability of transition between different statuses (Tang et al., 2015) is another technique to forecast PEVs load demand. For example, Zhou et al. (Zhou et al., 2017) applied grey-Markov chain to model PEV-TB considering the transition matrix among different states of PEVs charging procedure. The proposed method by Sun et al. (Sun et al., 2018) generates numerous scenarios via the MCS to determine the Markov transition matrix, that neglects the correlation between different travel parameters. Furthermore, to analyze the PEV-TB, the Markov method needs to group the status of PEVs' traveling into different steps. The computational limitation, therefore, arises since the number of steps should be increased to achieve an adequate level of accuracy in the results.

The third approach is based on the queuing theory. The method assumes a stochastic travel behavior and applies a homogeneous Poisson process to determine the arrival and departure rates of PEVs (Bae and Kwasinski, 2012; Bremermann et al., 2014; Kongjeen and Bhumkittipich, 2016; Li and Zhang, 2012; Vlachogiannis, 2009). For instance, Zhou et al. (Zhili Zhou and Tachun Lin, 2012) have integrate M/M/s queuing system with traffic flaw theory to estimate PEVs demand in the highway charging stations. The stochastic assumption, however, could decrease the accuracy of the results due to its inability to consider different factors for PEVs demand modeling. Furthermore, the queuing method cannot be effective in modeling the PEV-TB since it does not properly contemplate the State of Charge (SOC) condition of the PEV's battery. In one of the most recent studies, Hafez and Bhattacharya (Hafez and Bhattacharya, 2018), have resolved the previous shortcomings by using a non-homogeneous Poisson process and considering a more precise SOC in the PEV-TB modeling. This method, however, still does not consider the correlation between different travel parameters, which decreases the accuracy of the PEV-TB modeling.

The fourth approach is rooted in the trip chain and origin-destination (O-D) concepts from traffic studies. For instance, Wang et al., (Wang et al., 2014) have introduced a trip chain modeling in which the origin and destination, arrival and departure times, and trip length of the PEV trips are simulated. The existing studies calibrated the probability of transition between two consecutive time intervals based on the National Household Travel Survey (NTHS) data. Jianfeng et al. (Jianfeng et al., 2016) have proposed a MCS model for trip chain forecasting using probability distribution of NTHS data for three charging scenarios in weekend and weekdays. Mu et al. (Mu et al., 2014) have introduced a novel strategy for PEVs load forecasting at the nodes by O-D analysis. This trip chain method, however, is more suitable for conventional private vehicles which may have different travel pattern than PEVs and public transit fleet.

Artificial Neural Network (ANN) and machine learning methods are promising tools that can address the mentioned concerns in the PEVs load forecasting by deploying big data techniques. The ANN method identifies the parameters that influence the target (Zhou et al., 2019). In one of the few available studies, Panahi et al. (Panahi et al., 2015) have applied the conventional ANN method to forecast PEV-TB including arrival time and trip length. The findings, however, are not generalizable as the network sample is simplified and the data input is limited. Although the mentioned method utilized different probabilistic distribution function to train ANN, it decreases the accuracy of forecasting results since it uses the generated data with MCS to train the ANN. The conventional ANN does not forecast the objective with acceptable precision due to the high stochastic and non-linear behavior of PEV-TB. The rough ANN (R-ANN), therefore, is introduced to forecast different objective with high uncertainties such as wind speed (Shi et al., 2018), signature recognition (Elhoseny et al., 2018), load demand (Zhang et al., 2017), medical imaging (Hassanien et al., 2009; Ślęzak, 2006) and achieved acceptable results. This method boosts the efficiently of problems with uncertainties by considering the upper and lower bounds of the input variables since instead of point data it uses the interval data. For instance, Khodayar et al. (Khodayar et al., 2017) have discussed the feature of R-ANN in wind forecasting problems. The other applications of R-ANN in solving complex problems have been explained elsewhere (Ahmadi and Teshnehlab, 2017, Janjai et al., 2018). In this way, the R-ANN methods show their good ability to forecast the behavior of different phenomena with high uncertainty. This ability makes them

perfect choice in forecasting PEVs demand since the method considers the correlation between parameters to forecast trip length.

1.3. Paper contribution

The existing studies have applied stochastic and probabilistic methods such as Monte Carlo, queuing and Markov-chain to model and forecast PEV-TB. While these studies simplify the modeling by analyzing the effective parameters of PEV-TB independently, they ignore the correlation between different affecting parameters such as arrival time, departure time and trip length. Moreover, due to the fact that these methods are designed based on generating different scenarios, they have a lot of computational limitations which is more tangible with increasing the size of PEVs fleet. This paper aims to introduce a new approach to forecast the load demand posed to the power system by PEVs. The novel R-ANN method, despite other existing methods, preserves the correlation between arrival and departure time as well as trip length. The model first interdependently forecasts the arrival time and departure time of PEVs using historical data and then forecasts the trip length in correlation with arrival and departure times. Thus, the trip length, which is one of the most important parameters in modeling PEVs load demand, is estimated according to the arrival and departure time and the correlation between these variables is well-thought-out. To the best of our knowledge, this is the first study that applies artificial neural network based on rough structure to forecast PEV-TBs. The main contribution of our study is twofold: introducing a novel technique to forecast the PEV-TB based on R-ANN that considers the correlation of different parameters in PEV-TB modeling; and implementing the results of the proposed method in optimal charging algorithm and comparing with the conventional methods. We also compare our proposed method with MCS, the most common and benchmarking method used to forecast PEV-TB. Finally, we compare the aggregator cost under different simulation results.

The main contributions and innovations are summarized as follows:

- A novel technique is introduced to forecast the PEV-TB with high precision.
- The ANN with Rough neurons is implemented to deal with the uncertainty of input data.
- The recurrent structure is employed according to the dynamic behavior of understudy system.
- The correlation of the different travel behavior parameters is considered in forecasting PEV-TB.
- The aggregator's financial loss is calculated based on the accuracy of the forecasting PEV-TB.

1.4. Paper structure

The rest of the paper is organized as follows: first, optimal charging process and a brief description of ANN formulation based on conventional and rough structures are introduced. The numerical study section provides an explanation on the case study including PEV dataset and smart grid topology. Next, the simulation results are presented for various scenarios. Finally, the general conclusion about the simulation results and the recommended scheme are discussed.

2. METHODOLOGY

In this study, to estimate PEVs load demand on distribution network we propose an ANN based approach. The modeling framework contains two main parts: the first part presents an optimal charging algorithm and the second part presents the PEV-TB forecasting using the ANN method.

2.1. The proposed optimal charging procedure modeling

PEVs impose new challenges to power distribution networks including increasing line capacity congestion and power losses. In order to solve these problems, the optimal charging process should be applied. In this case, the optimal charging process is done by an intermediary entity called aggregator. The aggregator determines the PEV optimal charging pattern with forecasting the PEV-TB and electricity market prices. The main goal of the aggregator is to minimize the PEV total charging cost. In this section, the formulation for PEVs optimal charging problem is presented. The objective function in the optimization of PEVs smart charging is to minimize the Operation Cost (OC) subject to the network constraint:

$$OC = \sum_{t=1}^{24}\{ca(t) \times Ra(t) + Cr(t) \times Rr(t)\} + C_{inf} \quad (1)$$

Accordingly, load and generation equivalence has shown in equations (2) and (3) (Deilami et al., 2011):

$$\sum_t^{24} Ra(t) + \sum_t^{24} Wa(t) = \sum_t^{24} La(t) + \sum_t^{24} PEVa(t) + \sum_t^{24} Plossa(t) \quad (2)$$

$$\sum_t^{24} Rr(t) + \sum_t^{24} Wr(t) = \sum_t^{24} Lr(t) + \sum_t^{24} PEVr(t) + \sum_t^{24} Plossr(t) \quad (3)$$

The system active and reactive power loss are then extracted by equations (4) and (5) (Hafez and Bhattacharya, 2018):

$$Plossa(t) = \sum_{p=1}^{n} V(p,q,t) \times \sum_{q=1}^{n} V(p,q,t) \times \{G(p,q) \times \cos(\theta_{p,t} - \theta_{q,t}) + B(p,q) \times \sin(\theta_{p,t} - \theta_{q,t})\} \quad (4)$$

$$Plossr(t) = \sum_{p=1}^{n} V(p,q,t) \times \sum_{q=1}^{n} V(p,q,t) \times \{G(p,q) \times \cos(\theta_{p,t} - \theta_{q,t}) - B(p,q) \times \sin(\theta_{p,t} - \theta_{q,t})\} \quad (5)$$

Here, power and constraint of all equipment such as the voltage of nodes and frequency of system should not exceed the boundary values. Equipment's constraints are presented in equations (6) and (7):

$$P^u(t) \leq P^u_{max},\ Q^u(t) \leq Q^u_{max}\ \ u = 1,2,\dots,n_{eq} \quad (6)$$

$$V_{min} \leq V_p(t) \leq V_{\max}\ \ ,p = 1,2,\dots,n,\ \ t = 1,2,\dots,24 \quad (7)$$

Although several models are proposed for nonlinear SOC calculation by electrochemistry researchers, most of them are empirical-based models that are not proper for optimal operation of electric grids. Therefore, in this work, similar to the most of literature, a simplified linear equation is utilized for SOC calculation. Based on the PEV-TB data that forecasted by proposed ANN model, the initial State of Charge (SOC) of PEVs extracted by equation (8) (Ahmadian et al., 2018; Sedghi et al., 2016; Sun et al., 2018).

$$SOC_{init,l} = 100 - \frac{Tl_l}{C_{eff} \times Cap_{bat,l}} \times 100 \quad (8)$$

where, C_{eff} and $Cap_{bat,p}$ are obtained from ("Alternative Fuels Data Center," 2018) which provide annual selective information data about PEVs' characteristics..

One of the main constraints in PEVs charging modeling is to fulfil the minimum limitation of batteries' SOC at the departure time. This constraint is shown in equation (9):

$$SOC_{dep,l}\,(t\,) \geq SOC_{dep}, \qquad l = 1,2,3,\dots,n_{PEV} \tag{9}$$

Equation (10) declares that the SOC of PEVs at departure time have to be 100 percent of the whole battery capacity (Ahmadian et al., 2018; Xing et al., 2016).

$$SOC_l(t) = SOC_l(t-1) + P_l^{chr}(t) \times \rho_{chr} \tag{10}$$

The all electrical distribution network constraints are employed in the optimal charging procedure (Golshannavaz, 2018) which is defined as Non-Linear Programming (NLP)problem.

2.2. The proposed ANN theory

Forecasting PEV-TB requires handling huge datasets. We, therefore, need to adapt forecasting tools according to the huge size of datasets and using the data engineering tools such as ANN and machine learning methods. In ANN training, first we must identify the parameters that influence the target. These parameters are given as inputs for ANN training. One of the benefits of ANN is that after completing the training process, the network achievement is tested with a new data set and, given the accuracy of the results, the network performance can be verified. The structure of the ANN is designed according to the complexity of the under the study phenomenon. Indeed, the ANN acts like a Black Box, and once the network is completely trained and tested, it receives input data in the new situation to forecasts the target variable. Given that many parameters in PEV-TB problem that are correlated, the forecasting problem is highly complex. For instance, the drivers' travel behavior is irregular and arrival and departure times affect the trip length. In this regard, R-ANN can be appropriately applied to forecast PEV-TB.

In this section, a proposed R-ANN based model for forecasting PEV-TB is introduced. In this way, it has been assumed that intelligent communication infrastructure has been created between PEV owners and aggregators, who are in charge of controlling the charging pattern in an urban area. This communication system is being updated dynamically to train ANN data inputs to forecast the PEV actions. Figure 1 depicts the modeling framework of the proposed method. The framework utilizes previous drivers' arrival and departure times data to forecast the arrival time and departure time in the future. To train the ANN to forecast the arrival time and departure time for each travel category, the travel data are classified according to the behavioral similarity by the unsupervised k-means algorithm since the NHTS travel data are not classified based on different travel behaviors. In this regard, the arrival time and departure time variables have been independently analyzed using the R-ANN method. It must be noticed that the main goal of this approach is forecasting the trip length, which is required to determine the PEVs charging demand. On the other hand, to forecast the trip length, in addition to the historical data of trip length, we also employed the arrival time and departure time. In this paper, two common types of ANN training methods were applied to validate the results and accurately analyze the effects of R-ANNs.

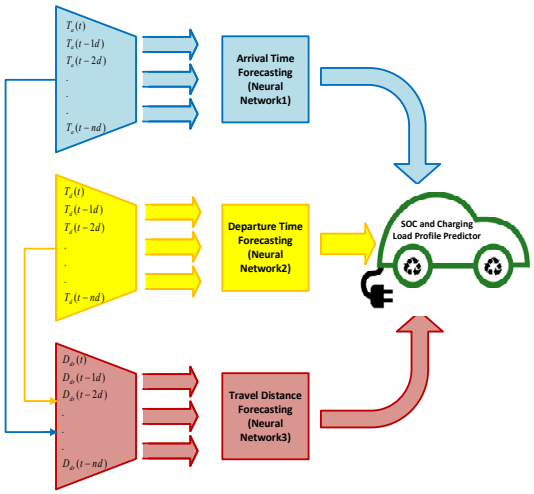

Figure 1: The proposed framework to model PEVs-TB

The formulation of the most common ANNs methods can be expressed in classic and Rough structures:

2.2.1. Classic ANN

The conventional ANN structure can be categorized into two groups:

2.2.1.1. Multilayer perceptron ANN with error back propagation learning method

The first ANN group is dubbed Multi-Layer Perceptron (MLP) neural network. In this structure, the Conventional Error Back Propagation (CEBP) algorithm based on gradient descent theory is used to train ANN (Li et al., 2012). The proposed ANN, which is depicted in Figure 2 has two layers, the activation functions of the first and second layers are defined as sigmoid and linear function, respectively. Feed-forward equations are defined as follows:

$$net_1^1(k) = (w_1^1(k))^T . X \quad (11)$$

$$net_2^1(k) = (w_2^1(k))^T . X \quad (12)$$

$$O^1(k) = [O_0^1(k), f_1^1(net_1^1(k)), f_2^1(net_2^1(k))]^T \quad (13)$$

$$net_1^2(k) = (w_1^2(k))^T . O^1(k) \quad (14)$$

$$O_1^2(k) = f_1^2(net_1^2(k)) \quad (15)$$

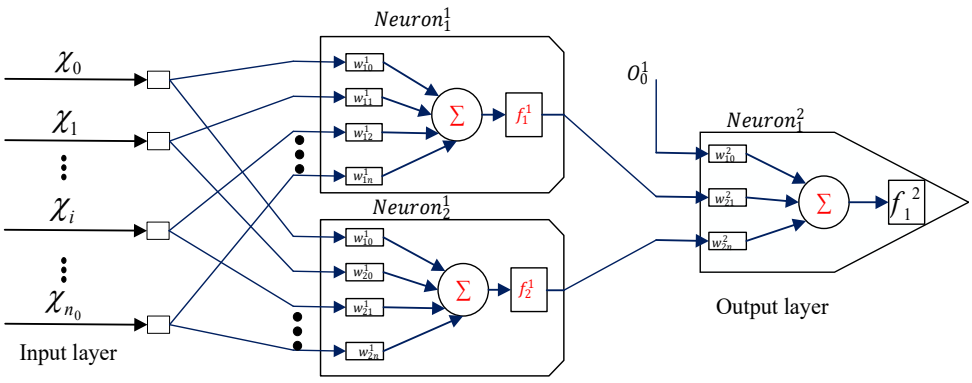

Figure 2: Multilayer perceptron neural network

According to the gradient descent method, the CEBP equations (learning strategy) are defined as follows:

$$\mathrm{E(k)} = \frac{1}{2}(e_1^2(k))^2 = \frac{1}{2}(d(k) - o_1^2(k))^2 = \frac{1}{2}(d(k) - f(net_1^2(k)))^2 \tag{16}$$

$$\nabla w_1^2\big(E(k)\big) = \frac{\partial E(k)}{\partial w_1^2(k)} = \frac{\partial E}{\partial net_1^2} \times \frac{\partial net_1^2}{\partial w_1^2}(k) \tag{17}$$

$$\nabla w_1^1\big(E(k)\big) = \frac{\partial E(k)}{\partial w_1^1(k)} = \frac{\partial E}{\partial net_1^2} \times \frac{\partial net_1^2}{\partial o_1^1} \times \frac{\partial o_1^1}{\partial net_1^1} \times \frac{\partial net_1^1}{\partial w_1^1}(k) \tag{18}$$

$$\nabla w_2^1\big(E(k)\big) = \frac{\partial E(k)}{\partial w_2^1(k)} = \frac{\partial E}{\partial net_1^2} \times \frac{\partial net_1^2}{\partial o_1^1} \times \frac{\partial o_1^1}{\partial net_2^1} \times \frac{\partial net_2^1}{\partial w_2^1}(k) \tag{19}$$

ANN weights are then updated as follows:

$$\Delta w_j^s(k) = -\eta_{\,w} \nabla w_j^s\big(E(k)\big) \tag{20}$$

$$\Delta w_j^s(k) = w_j^s(k+1) - w_j^s(k) = -\eta_{\,w} \nabla w_j^s\big(E(k)\big) \tag{21}$$

$$w_j^s(k+1) = w_j^s(k) - \eta_{\,w} \nabla w_j^s(E(k)) \tag{22}$$

The sigmoid function is the most common activation functions applied in ANNs. However, the function when faced with large inputs becomes saturated and disrupts the training of the ANN (Hikawa, 2003). The saturation condition reduces the accuracy and efficiency of the ANN. Using the activation function with flexible parameters is one way to avoid the saturation condition. By changing the parameters of the flexible functions, the behavior of these functions is reformed to prevent saturation during the training process. The Classic sigmoid activation function and *tanh* are expressed in equations (23) and (24). The flexible sigmoid and *tanh* activation function with more internal variables are then expressed in equations (25) and (26). Figures 3 and 4 show the behavior of flexible activation functions.

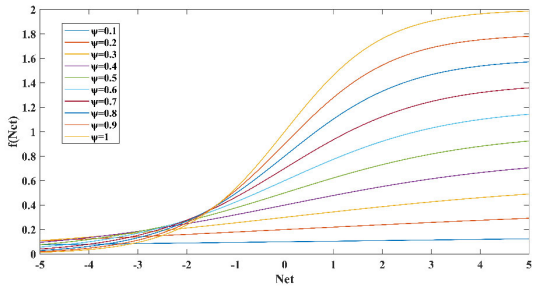

Figure 3: Flexible Sigmoid function for different values of ψ

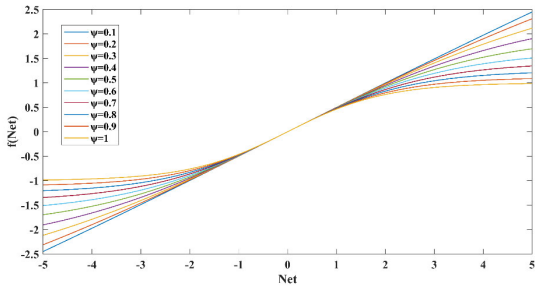

Figure 4: Flexible tanh function for different values of ψ

$$f\big(net(k)\big) = \frac{1}{1 + e^{-net(k)}} \tag{23}$$

$$f\big(net(k)\big) = \frac{1 - e^{-net(k)}}{1 + e^{-net(k)}} \tag{24}$$

$$f(net(k), \psi(k)) = \frac{2|\psi(k)|}{1 + e^{-net(k) \times \psi(k)}} \tag{25}$$

$$f(net(k), \psi(k)) = \frac{1}{\psi(k)} \times \frac{1 - e^{-net(k) \times \psi(k)}}{1 + e^{-net(k) \times \psi(k)}} \tag{26}$$

In this method, in addition to the weights, the coefficient of the activation functions (ψ) is trained. The formulations

for training the flexible activation function parameters are defined as follows:

$$\Delta\psi(k) = -\eta_\psi \times \frac{\partial E(k)}{\partial \psi(k)} \tag{27}$$

$$\psi(k+1) = \psi(k) + \eta_\psi \times \frac{\partial E(k)}{\partial \psi(k)} \tag{28}$$

2.2.1.2. Multilayer perceptron ANN based on Levenberg–Marquardt Training

The CEBP algorithm based on first-order derivative methods is the most popular training method of ANN. The second-order derivative method, however, significantly increases the speed of ANN training (Wilamowski and Yu, 2010). The LM strategy is then developed by combining the Newton and CEBP methods, which quickly forecasts more accurate results. While the Newton method uses the Hessian matrix, the LM method uses the Jacobian matrix. The Jacobian matrix is an approximated form of Hessian matrix which is shown in equation (29) (Lv et al., 2018), and LM method equations are defined in equation (30) (Behnood and Golafshani, 2018):

$$H(k) = \frac{\partial^2 E}{\partial w^2} = \nabla^2 E(k) = \begin{bmatrix} \frac{\partial^2 E}{\partial w_1^2} & \frac{\partial^2 E}{\partial w_2 \partial w_1} & \cdots & \frac{\partial^2 E}{\partial w_{N_w} \partial w_1} \\ \frac{\partial^2 E}{\partial w_1 \partial w_2} & \frac{\partial^2 E}{\partial w_2^2} & \cdots & \frac{\partial^2 E}{\partial w_{N_w} \partial w_2} \\ \vdots & \vdots & & \vdots \\ \frac{\partial^2 E}{\partial w_1 \partial w_{N_w}} & \frac{\partial^2 E}{\partial w_2 \partial w_{N_w}} & \cdots & \frac{\partial^2 E}{\partial w_{N_w}^2} \end{bmatrix} \tag{29}$$

$$H(k) \approx J(k)^T J(k) \tag{30}$$

Derived from the steepest descent method and Newton algorithm, the update rule of LM algorithm is proposed as:

$$\Delta w(k) = (J(k)^T J(k) + \mu(k) I(k))^{-1} J(k)^T e_{L-M}(k) \tag{31}$$

The Jacobian matrix and the error vector are then defined as:

$$J(k) = \begin{bmatrix} \frac{\partial e_{11}}{\partial w_1} & \frac{\partial e_{11}}{\partial w_2} & \cdots & \frac{\partial e_{11}}{\partial w_{N_w}} \\ \frac{\partial e_{12}}{\partial w_1} & \frac{\partial e_{12}}{\partial w_2} & \cdots & \frac{\partial e_{12}}{\partial w_{N_w}} \\ \cdots & \cdots & \cdots & \cdots \\ \frac{\partial e_{1M}}{\partial w_1} & \frac{\partial e_{1M}}{\partial w_2} & \cdots & \frac{\partial e_{1M}}{\partial w_{N_w}} \\ \cdots & \cdots & \cdots & \cdots \\ \frac{\partial e_{j1}}{\partial w_1} & \frac{\partial e_{j1}}{\partial w_2} & \cdots & \frac{\partial e_{j1}}{\partial w_{N_w}} \\ \frac{\partial e_{j2}}{\partial w_1} & \frac{\partial e_{j2}}{\partial w_2} & \cdots & \frac{\partial e_{j2}}{\partial w_{N_w}} \\ \cdots & \cdots & \cdots & \cdots \\ \frac{\partial e_{N_T M}}{\partial w_1} & \frac{\partial N_T M}{\partial w_2} & \cdots & \frac{\partial e_{N_T M}}{\partial w_{N_w}} \end{bmatrix} \quad e_{L-M}(k) = \begin{bmatrix} e_{11} \\ e_{12} \\ \cdots \\ e_{1M} \\ e_{j1} \\ e_{j2} \\ \cdots \\ e_{jM} \\ \cdots \\ e_{N_T 1} \\ e_{N_T 2} \\ \cdots \\ e_{N_T M} \end{bmatrix} \tag{32}$$

The training procedure is defined as follows (Lv et al., 2018):

$$w(k+1) = w(k) - \eta_w ((J^T(k) J(k) + \mu(k) I)^{-1} J^T(k) e_{L-M}(k) \tag{33}$$

In the LM method, the learning procedure is switched between Gauss-Newton and gradient descent methods. As

the magnitude of the $\mu(k)$ approaches zero, the LM switches to the Gauss-Newton method, and with increasing the $\mu(k)$ value, the LM switches to the gradient descent method (Lera and Pinzolas, 2002). The process starts with small $\mu(k)$ values to use the Gauss-Newton method and benefits from its high convergence speed. If a step does not yield to a smaller error, then it repeats the step with higher $\mu(k)$ until the error is decreased.

2.2.2. ANN based on Rough structures

In the study of real systems, due to the limitation of measuring instruments and environmental noise in input data, there is always uncertainty in the final results. Several studies have proposed different methods to scrutinize uncertainty in different phenomena. In an earlier study, Lingras (Lingras, 1996) introduced the Rough Neurons by combining the Rough structure with the ANN. Rough Neuron can be considered as a pair of neurons called upper and lower bounds. In Rough neurons, when x is considered as a feature variable, $\underline{x}$ and $\overline{x}$ are the lower and upper bounds, respectively.

2.2.2.1. Rough multilayer perceptron neural network with error back propagation learning method

Rough neuron configuration is depicted in Figure 5 and the proposed R-ANN is depicted in Figure 6. The complete formulation for a multi-layer perceptron ANN, whose hidden layer is considered as the Rough structure is expressed as follows:

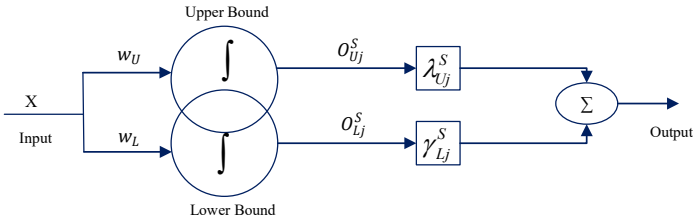

Figure 5: Rough neuron configuration

Feed forward equations are defined as follow (He et al., 2014):

$$net_{L_j}^s(k) = (w_{Lj}^1(k))^T.X \tag{34}$$

$$net_{U_j}^s(k) = (w_{Uj}^1(k))^T.X \tag{35}$$

For the rough multilayer perceptron neural network with error back propagation learning method, one hidden layer is considered.

$$O_{L_j}^s(k) = \min(f_j^s\left(net_{L_j}^s(k)\right), f_j^s\left(net_{U_j}^s(k)\right)) \tag{36}$$

$$O_{U_j}^s(k) = \max(f_j^s\left(net_{L_j}^s(k)\right), f_j^s\left(net_{U_j}^s(k)\right)) \tag{37}$$

$$O_j^s(k) = \gamma_j^s O_{L_j}^s(k) + \lambda_j^s O_{U_j}^s(k) \tag{38}$$

The $\gamma$and λ coefficients in equation (38) represent the effect of upper and lower bound values, respectively. Back Propagation equation (learning strategy), according to the gradient descent method, is applied to the learning process. The second layer is not Rough and its training strategy similar to the MLP with CEBP method and defined as (Ahmadi and Teshnehlab, 2017):

$$\Delta w_{ji}^{2}(k) = -\eta_w \frac{\partial E}{\partial w_{ji}^{2}}(k) \tag{39}$$

The first layer neurons are rough and have upper and lower bounds weights. They are trained in accordance with the following formulas:

$$\Delta w_{L_j}^{1} = -\eta_w \frac{\partial E}{\partial w_{L_j}^{1}}(k) = -\eta_w \times \frac{\partial E}{\partial e^2} \times \frac{\partial e^2}{\partial o^2} \times \frac{\partial o^2}{\partial net^2} \times \frac{\partial net^2}{\partial o_j^1} \times \frac{\partial o_j^1}{\partial o_{L_j}^1} \times \frac{\partial o_{L_j}^1}{\partial net_{L_j}^1} \times \frac{\partial net_{L_j}^1}{\partial w_{L_j}^1}(k) \tag{40}$$

$$\Delta w_{U_j}^{1} = -\eta_w \frac{\partial E}{\partial w_{U_j}^{1}}(k) = -\eta_w \times \frac{\partial E}{\partial e^2} \times \frac{\partial e^2}{\partial o^2} \times \frac{\partial o^2}{\partial net^2} \times \frac{\partial net^2}{\partial o_j^1} \times \frac{\partial o_j^1}{\partial o_{U_j}^1} \times \frac{\partial o_{U_j}^1}{\partial net_{U_j}^1} \times \frac{\partial net_{U_j}^1}{\partial w_{U_j}^1}(k) \tag{41}$$

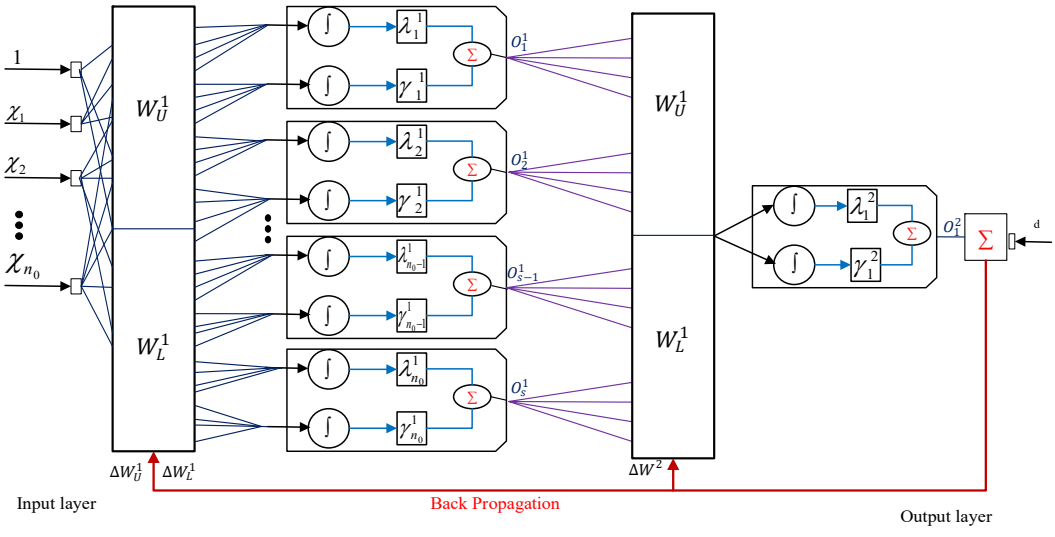

Figure 6: Rough MLP neural network with error back propagation learning method

2.2.2.2. Rough Multilayer perceptron neural network based on Levenberg–Marquardt Training

In this section, the combination of LM and Rough structure is applied. As previously stated, ANNs based on the Rough structure is effective in reducing noise and data uncertainty. In this method, the neurons of the middle layer are considered to be Rough. The training equations of the ANN's weights are the same as the Levenberg–Marquardt method, and the upper and lower neurons are trained through the second order derivative method. The Jacobian matrix based on Rough structure is defined as:

$$J(k) = \begin{bmatrix} \frac{\partial e_{11_u}}{\partial w_{1_u}} & \frac{\partial e_{11_u}}{\partial w_{2_u}} & \cdots & \frac{\partial e_{11_u}}{\partial w_{N_{w_u}}} \\ \frac{\partial e_{11_l}}{\partial w_{1_l}} & \frac{\partial e_{11_l}}{\partial w_{2_l}} & \cdots & \frac{\partial e_{11_l}}{\partial w_{N_{w_l}}} \\ \cdots & \cdots & \cdots & \cdots \\ \frac{\partial e_{1M_u}}{\partial w_{1_u}} & \frac{\partial e_{1M_u}}{\partial w_{2_u}} & \cdots & \frac{\partial e_{1M_u}}{\partial w_{N_{w_u}}} \\ \frac{\partial e_{1M_l}}{\partial w_{1_l}} & \frac{\partial e_{1M_l}}{\partial w_{2_l}} & \cdots & \frac{\partial e_{1M_l}}{\partial w_{N_{w_l}}} \\ \cdots & \cdots & \cdots & \cdots \\ \frac{\partial e_{N_T M_u}}{\partial w_{1_u}} & \frac{\partial e_{N_T M_u}}{\partial w_{2_u}} & \cdots & \frac{\partial e_{N_T M_u}}{\partial w_{N_{w_u}}} \\ \frac{\partial e_{N_T M_l}}{\partial w_{1_L}} & \frac{\partial e_{N_T M_l}}{\partial w_{2_L}} & \cdots & \frac{\partial e_{N_T M_l}}{w_{N_{w_L}}} \end{bmatrix} \quad e_{L-M}(k) = \begin{bmatrix} e_{11_u} \\ e_{11_l} \\ \cdots \\ e_{1M_u} \\ e_{1M_l} \\ \cdots \\ e_{N_T M_u} \\ e_{N_T M_l} \end{bmatrix} \tag{42}$$

2.2.3. Recurrent Artificial Neural Network based on Rough structures

The Recurrent Neural Networks, based on their structures, are capable of forecasting dynamic phenomena with high precision. The unique feedback loops in these configurations enable them to process sequences of data. They can process information in two directions: first, the flow of the information from initial input to final output, like feedforward neural networks and second, the feedback loop of information back into the network with backpropagation throughout the computational process.

2.2.3.1. Recurrent Rough multilayer perceptron neural network with error back propagation learning method

The Recurrent Rough Artificial Neural Network (RR-ANN) based on Elman structure has been shown in Fig. 7.

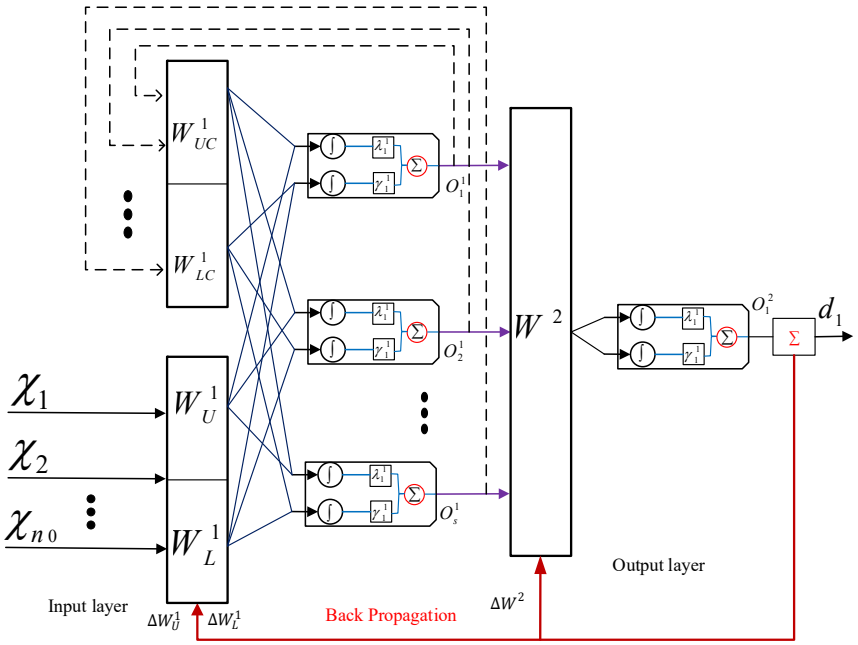

Figure 7: Recurrent Rough MLP neural network with error back propagation learning method

This structure, only contains a feed-forward network with additional units dubbed as context neurons. Context neurons receive input from the hidden layer neurons. Feed forward equations are defined as follows:

$$net_U^1(k) = W_U^1(k)X + W_{Uc}^1(k)X_c \tag{43}$$

$$net_L^1(k) = W_L^1(k)X + W_{Lc}^1(k)X_c \tag{44}$$

Other feed forward equations are defined as Rough networks in previous section. According to the CEBP equations, training procedure for the context neurons are considered as follows:

$$\Delta W_{Uc}^1(k) = -\eta_c \frac{\partial E(k)}{\partial W_{Uc}^1(k)} = -\eta_c \frac{\partial E}{\partial e}\frac{\partial e}{\partial O^2}\frac{\partial O^2}{\partial net^2}\frac{\partial Onet^2}{\partial O_U^1}\frac{\partial O_U^1}{\partial net_U^1}\frac{\partial net_U^1}{\partial W_{Uc}^1}(k) \tag{45}$$

$$\Delta W_{Lc}^1(k) = -\eta_c \frac{\partial E(k)}{\partial W_{Lc}^1(k)} = -\eta_c \frac{\partial E}{\partial e}\frac{\partial e}{\partial O^2}\frac{\partial O^2}{\partial net^2}\frac{\partial Onet^2}{\partial O_L^1}\frac{\partial O_L^1}{\partial net_L^1}\frac{\partial net_L^1}{\partial W_{Lc}^1}(k) \tag{46}$$

2.2.3.2. Recurrent Rough Multilayer perceptron neural network based on Levenberg–Marquardt Training

In RR-ANN the training procedure is same as Rough neurons but context neurons are added in the Jacobian matrix which increase the number of training parameters (Fu et al., 2015).

3. NUMERICAL STUDY

The PEV input dataset and smart grid topology are presented in this section.

3.1. PEV and power system dataset characteristics

To forecast the PEVs load demand, we use the roulette wheel technique (Cheng et al., 2016) to randomly allocate the type of PEVs to the network. The travel behavior is obtained based on the 2017 NHTS database ("National Household Travel Survey," 2018) including arrival and departure time and trip length. The market penetration rate for all PEVs models is also obtained from Alternative Fuels Data Center ("Alternative Fuels Data Center," 2018) which consists an all-inclusive information about US advanced transportation systems (Table 1). Furthermore, the battery capacity is selected according to the model of each PEV (Cheng et al., 2016).

Table 1: PEVs' Input Data ("Alternative Fuels Data Center," 2018)

PEV Model	Total Number	Battery capacity (kWh)	Max. Charging Rate(kWh)	PEV Model	Total Number	Battery capacity (kWh)	Max. Charging Rate(kWh)
Nissan LEAF	103,578	30	6.6	VW e-Golf	4,589	26.5	6.6
Tesla Model S	93,277	100	17.2	Mercedes B-Class E	3,312	36	10
BMW i3	24,721	42	7.4	Kia Soul EV	2,993	30.5	6.6
Fiat 500E	10,229	24	6.6	Mitsubishi i-MiEV	2,098	16	3.6
Chevrolet Spark	7,369	19	7.6	Honda Fit EV	1,071	20	6.6
Ford Focus EV	6,839	33.5	6.6	BMW Active E	965	33	6.4

The suggested methodology is applied to a distribution network feed by six 150 (KVA) wind turbines. For more details about the benchmark power system topology and its specifications, see (Carrano et al., 2007). The system information - load, electricity price - is obtained from Ontario Independent Electricity System Operator (IESO) ("The Independent Electricity System Operator (IESO)" 2017), Furthermore, the distribution network parameters have been gathered in 24 hours period for June, July and August 2018.

3.2. Error calculation criteria

To evaluate the accuracy and verification of the proposed ANN approach, three common different error criteria are implemented: the Mean absolute error (MAE), the Mean Absolute Percentage Error (MAPE) and the Root Mean Square Error (RMSE) (Yu et al., 2017).

$$MAE = \frac{1}{n_0}\sum_{g=1}^{n_0}\left(\left|\widehat{Y_g} - Y_g\right|\right) \tag{47}$$

$$MAPE = \frac{1}{n_0}\sum_{g=1}^{n_0}\left(\left|\widehat{Y_g} - Y_g\right|\right) \tag{48}$$

$$RMSE = \sqrt{\frac{1}{n_0}\sum_{g=1}^{n_0}\left(\left|\widehat{Y_g} - Y_g\right|\right)^2} \tag{49}$$

To further validate the simulation results the R-squared performance metric is also considered. R-square is a well-known metric in forecasting literature (Behnood and Golafshani, 2018; Golafshani and Behnood, 2018). The higher

R-squared value, implies the more accurate forecasting results. The R-squared is defined as follows (Yuan et al., 2018):

$$R^2 = 1 - \frac{\sum_{g=1}^{n_0}(Y_g - \hat{Y}_g)^2}{\sum_{g=1}^{n_0}(Y_g - \bar{Y}_g)^2} \quad (50)$$

The accuracy of the results depends on the initial weights values and since these values are randomly selected, in this study the training procedure has been performed 100 times and the best results are considered to determine the different error criteria. To avoid overfitting, the dropout technique has been employed during the training process (Srivastava et al., 2014).

4. RESULTS

Three scenarios are developed to evaluate the proposed method. The PEV-TB in each of the scenarios is forecasted using different ANNs methods (is done using MATLAB 9.3 software) and the optimal charging algorithm (the developed NLP problem is solved by CONOPT4 solver in GAMS software) is executed for a one-day period on a PC with an Intel Core i7, 3.4 GHz CPU and 16 GB of RAM. To verify the accuracy of the proposed method, the part of the data is considered not seen by the ANN during the training procedure and it is used as real data (Quan et al., 2014; Wang et al., 2017). In order to increase the accuracy of total imposed load on the distribution network, the intermittent behavior of load, price and wind power is considered by R-ANN techniques in PEV-TB simulation period.

4.1. Scenario 1

First, the traditional ANN is employed, where CEBP learning based on first-order derivative strategy and the Levenberg–Marquardt based on second-order derivative theory are applied to train ANN. The input data for network training is divided as follows: 80% of the data is used for network training, 10% for validation, and 10% for testing. The test results of the ANN training procedure are shown in Table 2.

Table 2: Different error criteria for scenario 1

Error criteria	CEBP			LM		
	Arrival time (hour)	Departure time (hour)	Trip Length (mile)	Arrival time (hour)	Departure time (hour)	Trip Length (mile)
MAE	5.33	3.68	11.33	4.43	2.69	9.09
RMSE	6.35	4.49	15.90	5.16	3.18	12.56
MAPE (%)	31.86	34.77	37.28	26.45	25.44	29.90

The accuracy of the results is then verified based on different error criteria. As shown in Table 2, the Levenberg–Marquardt method has a higher accuracy under different error criteria. The optimal charging algorithm is implemented for one day with the results obtained from different ANN methods and real data. The PEVs load is shown in Figure 8 for different modes.

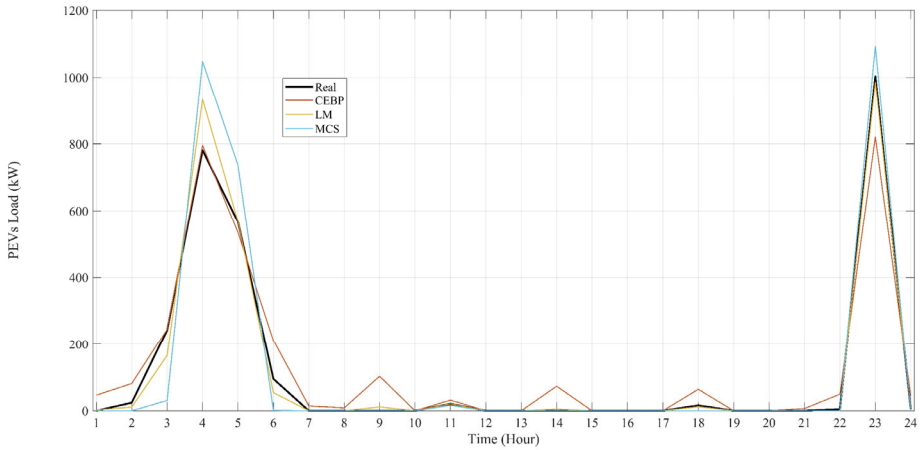

Figure 8: PEVs Load profiles for different forecasting methods in scenario 1

Levenberg–Marquardt learning method shows higher accuracy than CEBP learning method, but it still deviates significantly from the actual results obtained from real data. The difference between estimated and real PEVs load demand affect the aggregators benefits.

4.2. Scenario 2

In this section ANNs with the Rough structure have been used to forecast the PEV-TB. The Fragmentation of data into training, validation and testing is also similar to the previous scenario. The forecasting error of ANN with Rough structures are shown in Table 3.

Table 3: Different error criteria for scenario 2

Error criteria	R-CEBP			R-LM		
	Arrival time (hour)	Departure time (hour)	Trip Length (mile)	Arrival time (hour)	Departure time (hour)	Trip Length (mile)
MAE	4.12	2.53	7.84	1.81	2.90	5.87
RMSE	4.80	3.20	11.27	2.17	2.60	8.11
MAPE (%)	24.63	23.92	25.82	17.12	17.34	19.32

As can be seen from Table 3, the accuracy of the results has been improved compared to scenario 1. Same as the previous scenario, the PEVs load is shown in Figure 9 for different modes. By increasing the accuracy of forecasting PEV-TB, as shown in Figure 9, the imposed load on the power grid by PEVs is forecasted with more accuracy. This is important since the aggregators manage their proposed price in accordance with PEV owners and upstream distribution network based on forecasted PEV's load demand.

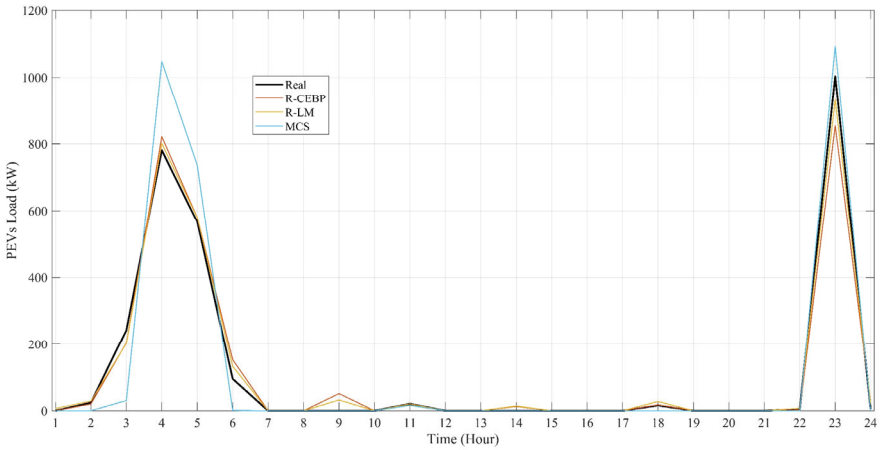

Figure 9: PEVs Load profiles for different forecasting methods in scenario 2

4.3. Scenario 3

In this part, RR-ANN have been utilized to forecast the PEV-TB. Division of data set are the same as previous scenarios. The forecasting errors are shown in Table 4.

Table 4: Different error criteria for scenario 3

Error criteria	RR-CEBP			RR-LM		
	Arrival time (hour)	Departure time (hour)	Trip Length (mile)	Arrival time (hour)	Departure time (hour)	Trip Length (mile)
MAE	2.15	3.45	6.42	1.68	2.43	5.48
RMSE	2.61	4.04	9.04	2.03	2.79	8.10
MAPE (%)	20.33	20.64	21.12	15.90	16.19	18.03

As shown in Table 4, employing recurrent structure resulted in about 2-3 % improvement in MAPE error criteria due to the ability of the recurrent network in forecasting behavior of the dynamic systems. The resultant PEVs load with different approaches is illustrated in Figure 10. As stated before, aggregator gains more profit using more precise method for forecasting PEV-TB.

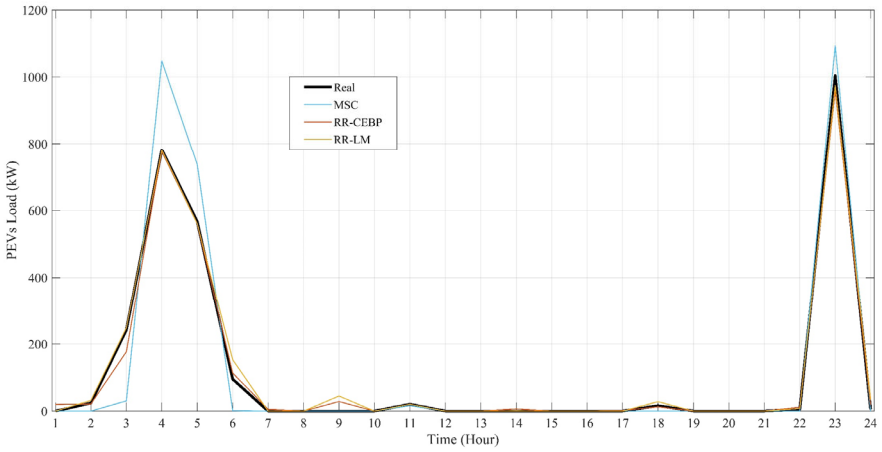

Figure 10: PEVs Load profiles for different forecasting methods in scenario 3

4.4. DISCUSSION

The simulation results show that the Levenberg–Marquardt method based on RR-ANN, which uses a second-order derivative to train and minimize the error rate, provides more accurate results compared to the other methods. In RR-ANNs, instead of using definite weights and neurons, interval weights are considered with rough neurons, and the internal loop from recurrent structure provided more accurate outcomes. An accurate evaluation of the different error criteria of the forecasting results presented in Tables 2-4 shows that employing ANN with Rough structure has a significant impact on improving the precision of the final results. Figures 11-13 compared the LM, R-LM and RR-LM results with MCS method and real data to show how considering the correlation between different variables such as arrival time, departure time and trip length can enhance the accuracy of PEVs load forecasting.

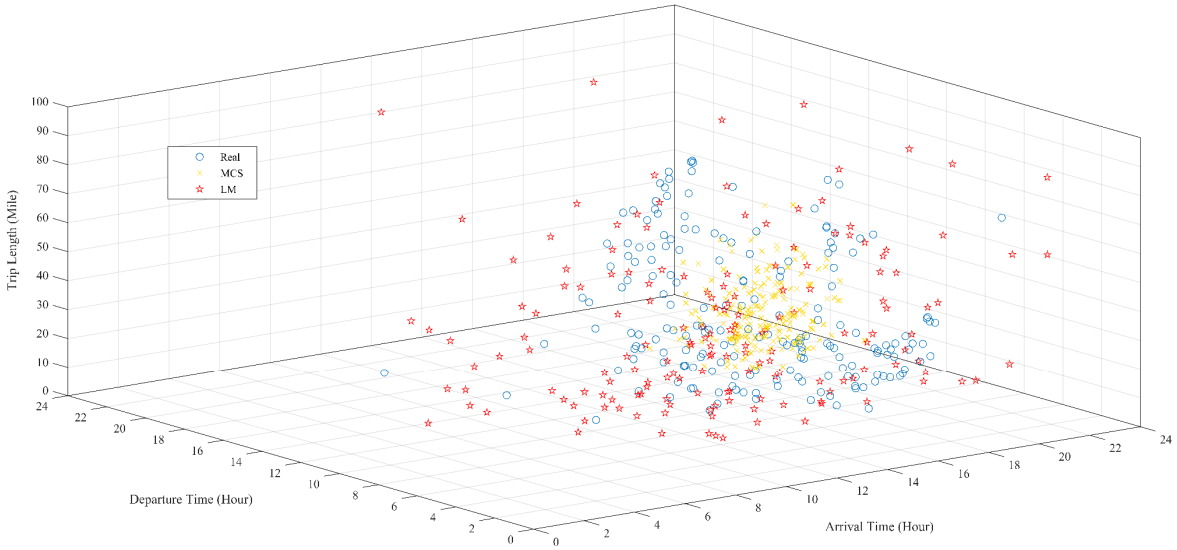

Figure 11: PEV-TB forecasting results for LM, MCS and real data

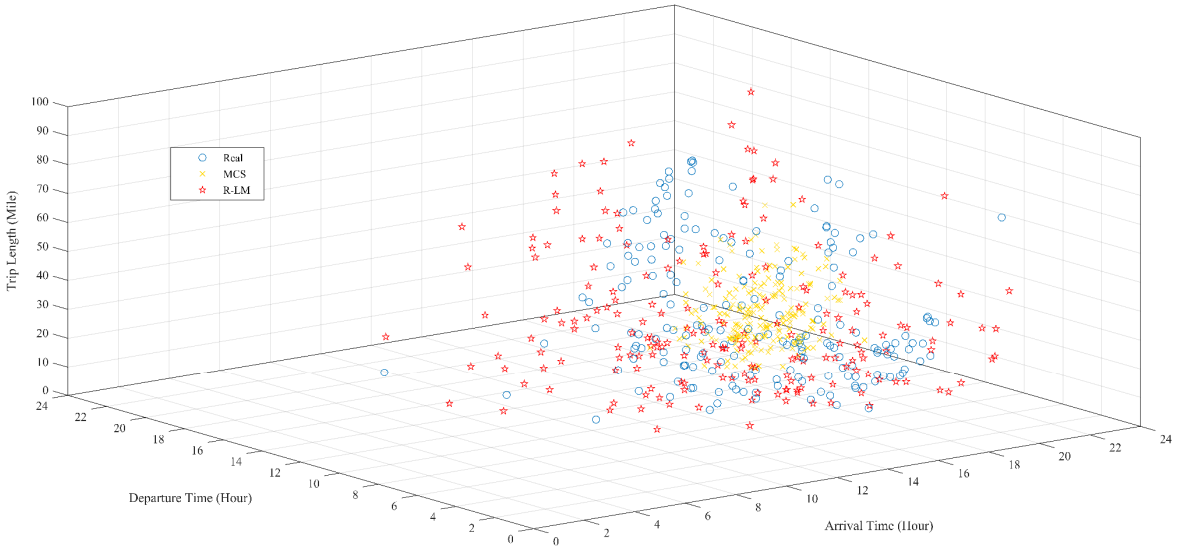

Figure 12: PEV-TB forecasting results for R-LM, MCS and real data

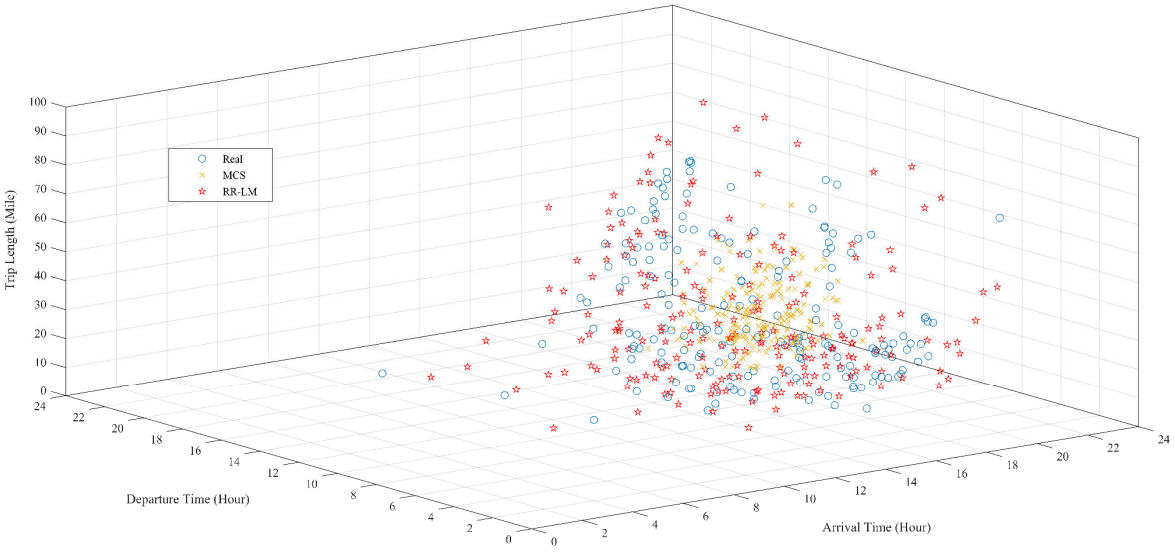

Figure 13: PEV-TB forecasting results for RR-LM, MCS and real data

As the results show, in the MCS method, which is a benchmark method in forecasting PEV-TB, the results are more focused around the mean value of data, since the correlation between different parameters is not considered. When the forecasting results are centralized around mean, the trips are very similar, and the variety of trips is very low, which could be very different from real trips topology and makes the aggregators to not have the accurate PEV-TB forecasting. The high tendency of forecasted trips around the average points would create fake high spikes in the PEVs optimal charging load profile, which do not happen in the reality. It has been also depicted in Figures 8-10, where forecasting PEV-TB with MCS increases the peaks of the PEVs load profile by 200kW compared to real trips. The proposed method, however, forecast the spikes in PEVs load profile more smoothly and closer to the real data. According to distribution network constraints and electric market policies, high spikes in PEVs load profile significantly affect the price of aggregators' purchasing power form upstream network.

For evaluating the forecasting results, R-squared performance metric is employed for the trip length as it is the most important parameter in PEV-TB (Figure 14). As the simulation results show, RR-LM has the highest R-squared value, 0.95. The results again emphasize on the influence of rough structure neurons on improving the performance of ANN method in forecasting travel behavior.

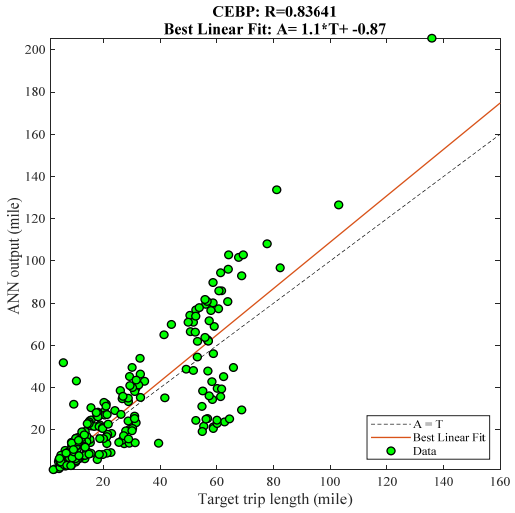

(a)

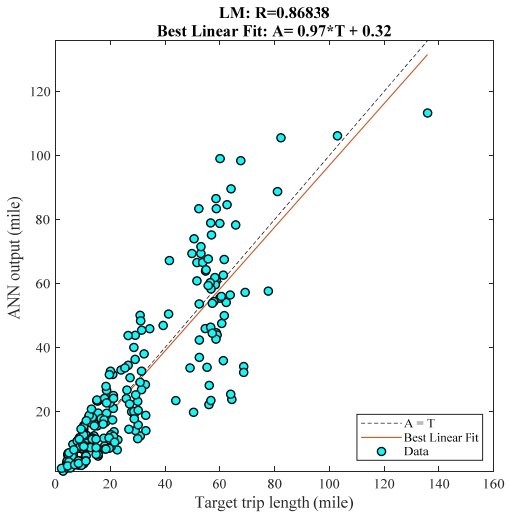

(b)

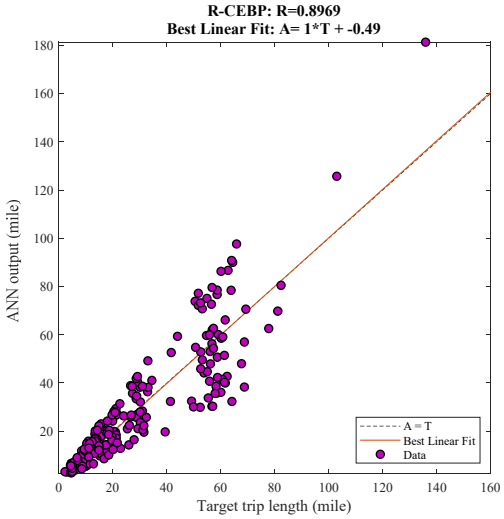

(c)

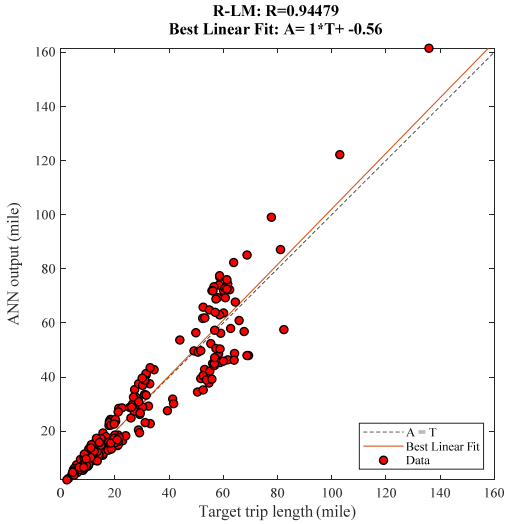

(d)

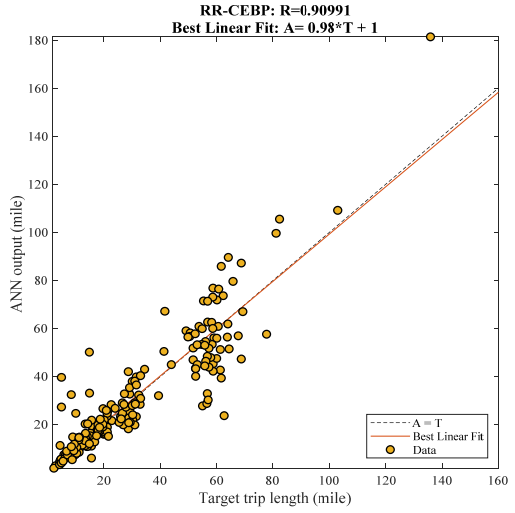

(e)

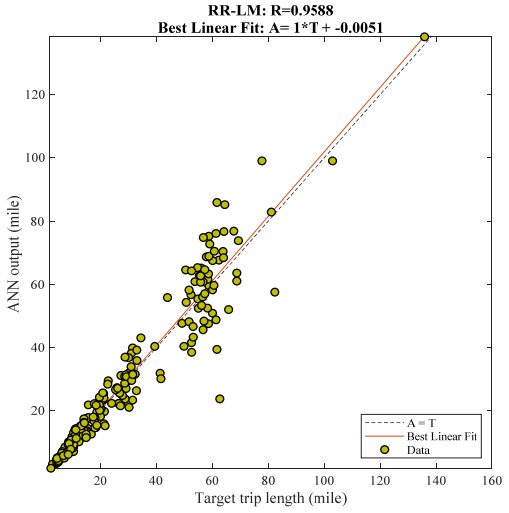

(f)

Figure 14: Trip length Regression between different method outputs and targets
(a): CEBP, (b): LM, (c): R-CEBP, (d): R-LM, (e): RR-CEBP, (f): RR-LM

The PEV-TB forecasting method while including the correlation of the various parameters by using the RR-LM method, is more consistent with the actual data than the LM method by itself. The PEV-TB forecasting results based on different ANN methods suggest using Rough based ANN with recurrent structure in the study of

phenomena with high uncertainty. By forecasting the PEV-TBs more precisely, we can envisage the PEVs imposed load on the network more accurately by up to 4.25 percent in comparison to MCS. The aggregator, therefore, would exchange energy with the upstream grid and PEV owners more meticulously. To elucidate the significance of this subject, Table 5 illustrates a complete comparison of cost of optimal charging procedure in different scenarios along with R-Squared values and average value of MAPE in different scenarios.

Table 5: Total results for scenarios 1-3 for 210 PEV in a day

Scenarios		Price ($)	Aggregator Financial Loss ($)	R-Squared for trip length forecasting	Average Forecasting error (MAPE%)
Real		3825.032	___	___	___
Scenario 1	CEBP	3849.809	24.777	0.83641	34.636
	LM	3817.754	7.277	0.86838	27.263
Scenario 2	R-CEBP	3830.478	5.446	0.89690	24.790
	R-LM	3829.465	4.432	0.94479	17.926
Scenario 3	RR-CEBP	3829.722	4.690	0.90991	20.696
	RR-LM	3829.151	4.119	0.95880	16.706
Monte Carlo		3811.283	13.749	___	___

To verify the proposed approach, the actual travel data are compared with the forecasted travel data by different methods from the cost perspective. As the results show, with the improvement in the forecasting of PEV-TB, the amount of aggregator financial loss is significantly reduced by up to 0.044 $/PEV in a day and about 16.06 $/PEV in a year; R-LM method compared to MCS. The average aggregator financial loss under the studied artificial intelligence-based method (CEBP, LM, R-CEBP, R-LM, RR-CEBP and RR-LM) can be reduced by 23% compared to the MCS. This is critical since the aggregators would have to pay to the upstream network or PEV owners in terms of the difference between the estimated and the actual price of PEV charging. Using the RR-ANN method in forecasting PEV-TB for 210 PEVs, reduces the aggregators' financial loss by $9.63 per day compared to the most common MCS method. Interestingly, employing rough structure neurons has a significant influence on the aggregator's financial loss. Considering the small sample size in our study, the actual financial loss in the real world would be much greater in a wider time-span. The practical implementation of the above method, in addition to the communication infrastructure for sending charge signals, requires a rich database. Since our proposed method is a data-driven approach, the data plays an essential role in its real-world implication. Therefore, it is necessary to utilize new macroscopic methods to obtain the travel behavior parameters of the region understudy (Amirgholy and Gao, 2017). These data sets are usually available through local transportation agencies. Hence, with sufficient amount of data, our proposed method can be applied in real distribution systems. Afterwards, a sophisticated data processing center is required in order to employ the proposed artificial intelligent approach and optimal charging procedure.

5. CONCLUSION

In this paper, Rough Artificial Neural Network (R-ANN) approach was applied to forecast the Plug-in Electric Vehicles Travel Behavior (PEVs-TB) and the PEVs load on the distribution network. Given the ability of the R-ANNs in analyzing phenomena with high uncertainty, they can improve the accuracy of forecasting results. Employing the rough neurons in recurrent based network improved the forecasting accuracy considering the

dynamic behavior of the system. In addition, in this paper, two training methods, Conventional Error Back Propagation (CEBP) and Levenberg–Marquardt, are utilized which are defined based on first and second order derivatives, respectively. The results showed that Levenberg–Marquardt method is more accurate in PEVs-TB. To investigate the importance of accurate forecasting of PEV-TB, optimal charging procedure was performed in different modes. The results showed that by using Recurrent Rough Artificial Neural Network (RR-ANN), the aggregator could forecast PEV-TB and PEVs load more accurately than Monte Carlo Simulation (MCS) which is a benchmarking method in this field and gains more efficient operating profit. In fact, forecasting the PEV-TB for the aggregator is very important, since the greater the difference between the forecasted cost and the real value, the aggregator should spend more money on the upstream distribution network or PEV owners, which will reduce the aggregator's profit. Results from our study recommend using rough based networks to forecast the PEV-TB in contemplation of investigating the PEV optimal charging problem from the aggregators' point of view. The findings imply the importance of accurate forecasting of PEVs' load demand on the network in order to moderate the PEVs' charging cost and help to increase the penetration of PEVs in the transportation fleet.

6. REFERENCES

Ahmadi, G., Teshnehlab, M., 2017. Designing and implementation of stable sinusoidal rough-neural identifier. IEEE Trans. neural networks Learn. Syst. 28, 1774–1786.

Ahmadian, A., Sedghi, M., Mohammadi-Ivatloo, B., Elkamel, A., Aliakbar Golkar, M., Fowler, M., 2018. Cost-Benefit Analysis of V2G Implementation in Distribution Networks Considering PEVs Battery Degradation. IEEE Trans. Sustain. Energy. https://doi.org/10.1109/TSTE.2017.2768437

Aliasghari, P., Mohammadi-Ivatloo, B., Alipour, M., Abapour, M., Zare, K., 2018. Optimal scheduling of plug-in electric vehicles and renewable micro-grid in energy and reserve markets considering demand response program. J. Clean. Prod. 186, 293–303.

Alternative Fuels Data Center [WWW Document], 2018. URL https://afdc.energy.gov/data/10567 (accessed 12.5.18).

Amirgholy, M., Gao, H.O., 2017. Modeling the dynamics of congestion in large urban networks using the macroscopic fundamental diagram: User equilibrium, system optimum, and pricing strategies. Transp. Res. Part B Methodol. https://doi.org/10.1016/j.trb.2017.07.006

Arias, M.B., Bae, S., 2016. Electric vehicle charging demand forecasting model based on big data technologies. Appl. Energy 183, 327–339. https://doi.org/10.1016/J.APENERGY.2016.08.080

Bae, S., Kwasinski, A., 2012. Spatial and Temporal Model of Electric Vehicle Charging Demand. IEEE Trans. Smart Grid 3, 394–403. https://doi.org/10.1109/TSG.2011.2159278

Behnood, A., Golafshani, E.M., 2018. Predicting the compressive strength of silica fume concrete using hybrid artificial neural network with multi-objective grey wolves. J. Clean. Prod. https://doi.org/10.1016/j.jclepro.2018.08.065

Biswas, P.P., Suganthan, P.N., Amaratunga, G.A.J., 2017. Optimal power flow solutions incorporating stochastic wind and solar power. Energy Convers. Manag. 148, 1194–1207. https://doi.org/10.1016/J.ENCONMAN.2017.06.071

Bremermann, L.E., Matos, M., Lopes, J.A.P., Rosa, M., 2014. Electric vehicle models for evaluating the security of supply. Electr. Power Syst. Res. 111, 32–39. https://doi.org/10.1016/J.EPSR.2014.02.001

Carrano, E.G., Guimarães, F.G., Takahashi, R.H.C., Neto, O.M., Campelo, F., 2007. Electric distribution network expansion under load-evolution uncertainty using an immun system inspired algorithm. IEEE Trans. Power Syst. https://doi.org/10.1109/TPWRS.2007.894847

Cheng, Y.-S., Chuang, M.-T., Liu, Y.-H., Wang, S.-C., Yang, Z.-Z., 2016. A particle swarm optimization based power dispatch algorithm with roulette wheel re-distribution mechanism for equality constraint. Renew.

Energy 88, 58–72. https://doi.org/10.1016/J.RENENE.2015.11.023

Deilami, S., Masoum, A.S., Moses, P.S., Masoum, M.A.S., 2011. Real-time coordination of plug-in electric vehicle charging in smart grids to minimize power losses and improve voltage profile. IEEE Trans. Smart Grid 2, 456–467. https://doi.org/10.1109/TSG.2011.2159816

Elhoseny, M., Nabil, A., Hassanien, A.E., Oliva, D., 2018. Hybrid rough neural network model for signature recognition, in: Advances in Soft Computing and Machine Learning in Image Processing. Springer, pp. 295–318.

Fan, Y. Van, Perry, S., Klemeš, J.J., Lee, C.T., 2018. A review on air emissions assessment: Transportation. J. Clean. Prod. 194, 673–684. https://doi.org/10.1016/J.JCLEPRO.2018.05.151

Fu, X., Li, S., Fairbank, M., Wunsch, D.C., Alonso, E., 2015. Training Recurrent Neural Networks with the Levenberg-Marquardt Algorithm for Optimal Control of a Grid-Connected Converter. IEEE Trans. Neural Networks Learn. Syst. https://doi.org/10.1109/TNNLS.2014.2361267

Golafshani, E.M., Behnood, A., 2018. Application of soft computing methods for predicting the elastic modulus of recycled aggregate concrete. J. Clean. Prod. https://doi.org/10.1016/j.jclepro.2017.11.186

Golshannavaz, S., 2018. Cooperation of electric vehicle and energy storage in reactive power compensation: An optimal home energy management system considering PV presence. Sustain. Cities Soc. https://doi.org/10.1016/j.scs.2018.02.018

Hafez, O., Bhattacharya, K., 2018. Queuing analysis based PEV load modeling considering battery charging behavior and their impact on distribution system operation. IEEE Trans. Smart Grid. https://doi.org/10.1109/TSG.2016.2550219

He, Z., Lin, S., Deng, Y., Li, X., Qian, Q., 2014. A rough membership neural network approach for fault classification in transmission lines. Int. J. Electr. Power Energy Syst. 61, 429–439.

Hikawa, H., 2003. A new digital pulse-mode neuron with adjustable activation function. IEEE Trans. Neural Networks 14, 236–242. https://doi.org/10.1109/TNN.2002.804312

Janjai, S., Tohsing, K., Lamlert, N., Mundpookhier, T., Chanalert, W., Bala, B.K., 2018. Experimental performance and artificial neural network modeling of solar drying of litchi in the parabolic greenhouse dryer. J. Renew. Energy Smart Grid Technol. 13.

Jianfeng, W., Xiangning, X., Jian, Z., Kunyu, L., Yang, Y., Shun, T., 2016. Charging demand for electric vehicle based on stochastic analysis of trip chain. IET Gener. Transm. Distrib. 10, 2689–2698. https://doi.org/10.1049/iet-gtd.2015.0995

Khodayar, M., Kaynak, O., Khodayar, M.E., 2017. Rough Deep Neural Architecture for Short-Term Wind Speed Forecasting. IEEE Trans. Ind. Informatics 13, 2770–2779.

Kongjeen, Y., Bhumkittipich, K., 2016. Modeling of electric vehicle loads for power flow analysis based on PSAT, in: 2016 13th International Conference on Electrical Engineering/Electronics, Computer, Telecommunications and Information Technology (ECTI-CON). IEEE, pp. 1–6. https://doi.org/10.1109/ECTICon.2016.7561430

Lera, G., Pinzolas, M., 2002. Neighborhood based Levenberg-Marquardt algorithm for neural network training. IEEE Trans. neural networks 13, 1200–1203.

Li, G., Zhang, X.-P., 2012. Modeling of Plug-in Hybrid Electric Vehicle Charging Demand in Probabilistic Power Flow Calculations. IEEE Trans. Smart Grid 3, 492–499. https://doi.org/10.1109/TSG.2011.2172643

Li, J., Cheng, J., Shi, J., Huang, F., 2012. Brief Introduction of Back Propagation (BP) Neural Network Algorithm and Its Improvement. Springer, Berlin, Heidelberg, pp. 553–558. https://doi.org/10.1007/978-3-642-30223-7_87

Li, X., Zhang, Q., Peng, Z., Wang, A., Wang, W., 2019. A data-driven two-level clustering model for driving pattern analysis of electric vehicles and a case study. J. Clean. Prod. 206, 827–837.

Lingras, P., 1996. Rough neural networks, in: Proc. of the 6th Int. Conf. on Information Processing and Management of Uncertainty in Knowledgebased Systems. pp. 1445–1450.

Lv, C., Xing, Y., Zhang, J., Na, X., Li, Y., Liu, T., Cao, D., Wang, F.-Y., 2018. Levenberg–Marquardt Backpropagation Training of Multilayer Neural Networks for State Estimation of a Safety-Critical Cyber-

Physical System. IEEE Trans. Ind. Informatics 14, 3436–3446.

Mohseni-Bonab, S.M., Rabiee, A., 2017. Optimal reactive power dispatch: A review, and a new stochastic voltage stability constrained multi-objective model at the presence of uncertain wind power generation. IET Gener. Transm. Distrib. https://doi.org/10.1049/iet-gtd.2016.1545

Morshed, M.J., Hmida, J. Ben, Fekih, A., 2018. A probabilistic multi-objective approach for power flow optimization in hybrid wind-PV-PEV systems. Appl. Energy 211, 1136–1149. https://doi.org/10.1016/J.APENERGY.2017.11.101

Mu, Y., Wu, J., Jenkins, N., Jia, H., Wang, C., 2014. A Spatial–Temporal model for grid impact analysis of plug-in electric vehicles. Appl. Energy 114, 456–465. https://doi.org/10.1016/J.APENERGY.2013.10.006

Mukherjee, J.C., Gupta, A., 2017. Distributed charge scheduling of plug-in electric vehicles using inter-aggregator collaboration. IEEE Trans. Smart Grid 8, 331–341.

National Household Travel Survey [WWW Document], 2018. URL https://nhts.ornl.gov/ (accessed 12.5.18).

Neaimeh, M., Wardle, R., Jenkins, A.M., Yi, J., Hill, G., Lyons, P.F., Hübner, Y., Blythe, P.T., Taylor, P.C., 2015. A probabilistic approach to combining smart meter and electric vehicle charging data to investigate distribution network impacts. Appl. Energy 157, 688–698. https://doi.org/10.1016/J.APENERGY.2015.01.144

Panahi, D., Deilami, S., Masoum, M.A.S., Islam, S.M., 2015. Forecasting plug-in electric vehicles load profile using artificial neural networks, in: 2015 Australasian Universities Power Engineering Conference (AUPEC). IEEE, pp. 1–6. https://doi.org/10.1109/AUPEC.2015.7324879

Qian, K., Zhou, C., Allan, M., Yuan, Y., 2011. Modeling of Load Demand Due to EV Battery Charging in Distribution Systems. IEEE Trans. Power Syst. 26, 802–810. https://doi.org/10.1109/TPWRS.2010.2057456

Quan, H., Srinivasan, D., Khosravi, A., 2014. Short-term load and wind power forecasting using neural network-based prediction intervals. IEEE Trans. neural networks Learn. Syst. 25, 303–315.

Sedghi, M., Ahmadian, A., Aliakbar-Golkar, M., 2016. Optimal storage planning in active distribution network considering uncertainty of wind power distributed generation. IEEE Trans. Power Syst. https://doi.org/10.1109/TPWRS.2015.2404533

Shi, Z., Liang, H., Dinavahi, V., 2018. Direct interval forecast of uncertain wind power based on recurrent neural networks. IEEE Trans. Sustain. Energy 9, 1177–1187.

Srivastava, N., Hinton, G., Krizhevsky, A., Sutskever, I., Salakhutdinov, R., 2014. Dropout: A Simple Way to Prevent Neural Networks from Overfitting. J. Mach. Learn. Res. https://doi.org/10.1214/12-AOS1000

Sun, S., Yang, Q., Yan, W., 2018. A Novel Markov-Based Temporal-SoC Analysis for Characterizing PEV Charging Demand. IEEE Trans. Ind. Informatics 14, 156–166. https://doi.org/10.1109/TII.2017.2720694

Sun, S., Yang, Q., Yan, W., 2016. A novel statistical Markov-based approach for modeling charging demand of plug-in electric vehicles, in: 2016 China International Conference on Electricity Distribution (CICED). IEEE, pp. 1–6. https://doi.org/10.1109/CICED.2016.7576348

Tang, J., Brouste, A., Tsui, K.L., 2015. Some improvements of wind speed Markov chain modeling. Renew. Energy 81, 52–56. https://doi.org/10.1016/J.RENENE.2015.03.005

Tayarani, M., Nadafianshahamabadi, R., Poorfakhraei, A., Rowangould, G., 2018a. Evaluating the cumulative impacts of a long range regional transportation plan: Particulate matter exposure, greenhouse gas emissions, and transportation system performance. Transp. Res. Part D Transp. Environ. 63, 261–275. https://doi.org/10.1016/j.trd.2018.05.014

Tayarani, M., Poorfakhraei, A., Nadafianshahamabadi, R., Rowangould, G., 2018b. Can regional transportation and land-use planning achieve deep reductions in GHG emissions from vehicles? Transp. Res. Part D Transp. Environ. 63, 222–235. https://doi.org/10.1016/J.TRD.2018.05.010

The Independent Electricity System Operator (IESO) [WWW Document], 2018. URL http://ieso.ca/ (accessed 12.5.18).

US EPA, 2019. Smog, Soot, and Other Air Pollution from Transportation [WWW Document]. URL https://www.epa.gov/transportation-air-pollution-and-climate-change/smog-soot-and-local-air-pollution (accessed 1.7.19).

Vlachogiannis, J.G., 2009. Probabilistic Constrained Load Flow Considering Integration of Wind Power Generation and Electric Vehicles. IEEE Trans. Power Syst. 24, 1808–1817. https://doi.org/10.1109/TPWRS.2009.2030420

Wang, D., Guan, X., Wu, J., Gao, J., 2014. Analysis of multi-location PEV charging behaviors based on trip chain generation, in: 2014 IEEE International Conference on Automation Science and Engineering (CASE). IEEE, pp. 151–156. https://doi.org/10.1109/CoASE.2014.6899319

Wang, L., Zhang, Z., Chen, J., 2017. Short-Term Electricity Price Forecasting with Stacked Denoising Autoencoders. IEEE Trans. Power Syst. 32, 2673–2681.

Wang, Y., Infield, D., 2018. Markov Chain Monte Carlo simulation of electric vehicle use for network integration studies. Int. J. Electr. Power Energy Syst. 99, 85–94. https://doi.org/10.1016/J.IJEPES.2018.01.008

Wilamowski, B.M., Yu, H., 2010. Improved computation for Levenberg–Marquardt training. IEEE Trans. neural networks 21, 930–937.

Xing, H., Fu, M., Lin, Z., Mou, Y., 2016. Decentralized Optimal Scheduling for Charging and Discharging of Plug-In Electric Vehicles in Smart Grids. IEEE Trans. Power Syst. 31, 4118–4127. https://doi.org/10.1109/TPWRS.2015.2507179

Yang, Q., Sun, S., Deng, S., Zhao, Q., Zhou, M., 2018. Optimal sizing of PEV fast charging stations with Markovian demand characterization. IEEE Trans. Smart Grid 1–1. https://doi.org/10.1109/TSG.2018.2860783

Yu, C., Li, Y., Zhang, M., 2017. Comparative study on three new hybrid models using Elman Neural Network and Empirical Mode Decomposition based technologies improved by Singular Spectrum Analysis for hour-ahead wind speed forecasting. Energy Convers. Manag. 147, 75–85. https://doi.org/10.1016/j.enconman.2017.05.008

Yu, L., Zhao, T., Chen, Q., Zhang, J., 2015. Centralized bi-level spatial-temporal coordination charging strategy for area electric vehicles. CSEE J. Power Energy Syst. 1, 74–83. https://doi.org/10.17775/CSEEJPES.2015.00050

Yuan, J., Farnham, C., Azuma, C., Emura, K., 2018. Predictive artificial neural network models to forecast the seasonal hourly electricity consumption for a University Campus. Sustain. Cities Soc. https://doi.org/10.1016/j.scs.2018.06.019

Zhang, T., Liu, D., Yue, D., 2017. Rough neuron based rbf neural networks for short-term load forecasting, in: Energy Internet (ICEI), IEEE International Conference On. IEEE, pp. 291–295.

Zhili Zhou, Tachun Lin, 2012. Spatial and Temporal Model for Electric Vehicle rapid charging demand, in: 2012 IEEE Vehicle Power and Propulsion Conference. IEEE, pp. 345–348. https://doi.org/10.1109/VPPC.2012.6422675

Zhou, Y., Chang, F.J., Chang, L.C., Kao, I.F., Wang, Y.S., 2019. Explore a deep learning multi-output neural network for regional multi-step-ahead air quality forecasts. J. Clean. Prod. https://doi.org/10.1016/j.jclepro.2018.10.243

Zhou, Y., Qi, B., Zhang, B., 2017. Online prediction of electrical load for distributed management of PEV based on Grey-Markov model, in: 2017 29th Chinese Control And Decision Conference (CCDC). IEEE, pp. 6911–6916. https://doi.org/10.1109/CCDC.2017.7978426